ADVANCED HEALTHCARE MATERIALS
www.advhealthmat.de

Biodegradable, Self-Reinforcing Vascular Grafts for In Situ Tissue Engineering Approaches

*Sabrina Rohringer, Christian Grasl, Katharina Ehrmann, Pia Hager, Clemens Hahn, Sophie J. Specht, Ingrid Walter, Karl H. Schneider, Lydia M. Zopf, Stefan Baudis, Robert Liska, Heinrich Schima, Bruno K. Podesser, and Helga Bergmeister**

Clinically available small-diameter synthetic vascular grafts (SDVGs) have unsatisfactory patency rates due to impaired graft healing. Therefore, autologous implants are still the gold standard for small vessel replacement. Bioresorbable SDVGs may be an alternative, but many polymers have inadequate biomechanical properties that lead to graft failure. To overcome these limitations, a new biodegradable SDVG is developed to ensure safe use until adequate new tissue is formed. SDVGs are electrospun using a polymer blend composed of thermoplastic polyurethane (TPU) and a new self-reinforcing TP(U-urea) (TPUU). Biocompatibility is tested in vitro by cell seeding and hemocompatibility tests. In vivo performance is evaluated in rats over a period for up to six months. Autologous rat aortic implants serve as a control group. Scanning electron microscopy, micro-computed tomography (μCT), histology, and gene expression analyses are applied. TPU/TPUU grafts show significant improvement of biomechanical properties after water incubation and exhibit excellent cyto- and hemocompatibility. All grafts remain patent, and biomechanical properties are sufficient despite wall thinning. No inflammation, aneurysms, intimal hyperplasia, or thrombus formation are observed. Evaluation of graft healing shows similar gene expression profiles of TPU/TPUU and autologous conduits. These new biodegradable, self-reinforcing SDVGs may be promising candidates for clinical use in the future.

1. Introduction

Treatment of life-threatening cardiovascular disease often requires replacement of compromised blood vessels. Autologous tissues such as the internal mammary artery or great saphenous vein are considered the gold standard for coronary and peripheral bypass grafting. However, in patients with concomitant diseases or previous vascular harvesting, the use of autografts is often not indicated.[1–3] Clinically approved grafts made of polyethylene terephthalate (PET) or expanded polytetrafluorethylene (ePTFE) have satisfactory long-term patency rates for the replacement of large vessels but they do not perform adequately as small-diameter vascular grafts.[2,4] Therefore, there is a significant need for the development of new synthetic replacement materials. Numerous studies have described the performance of various tissue-engineered SDVGs in pre-clinical studies,[5] but only a few made the transition to the clinic, either as pulmonary artery conduits for congenital heart defects[6] or as arteriovenous grafts for hemodialysis access.[7–9] A major reason for graft failure remains the biomechanical mismatch between the conduit and the native blood vessel.[10,11] More elastic

S. Rohringer, K. Ehrmann, P. Hager, C. Hahn, S. J. Specht, K. H. Schneider, B. K. Podesser, H. Bergmeister
Center for Biomedical Research and Translational Surgery
Medical University of Vienna
Waehringer Gürtel 18-20, Vienna 1090, Austria
E-mail: helga.bergmeister@meduniwien.ac.at

The ORCID identification number(s) for the author(s) of this article can be found under https://doi.org/10.1002/adhm.202300520

DOI: 10.1002/adhm.202300520

S. Rohringer, K. Ehrmann, K. H. Schneider, L. M. Zopf, S. Baudis, R. Liska, B. K. Podesser, H. Bergmeister
Austrian Cluster for Tissue Regeneration
Donaueschingenstraße 13, Vienna 1200, Austria

S. Rohringer, C. Grasl, P. Hager, C. Hahn, S. J. Specht, K. H. Schneider, H. Schima, B. K. Podesser, H. Bergmeister
Ludwig Boltzmann Institute for Cardiovascular Research
Waehringer Gürtel 18-20, Vienna 1090, Austria

C. Grasl, H. Schima
Center for Medical Physics and Biomedical Engineering
Medical University of Vienna
Waehringer Gürtel 18-20, Vienna 1090, Austria

K. Ehrmann, S. Baudis, R. Liska
Institute of Applied Synthetic Chemistry
Technical University of Vienna
Getreidemarkt 9/163, Vienna 1060, Austria

polymers have been developed to overcome this problem. As early as 1989, Hayashi et al. described favorable biomechanical properties of polyurethane vascular prostheses surrounded by a polyester mesh.[12] Thermoplastic polyurethanes are biocompatible and allow tuning of biomechanical features by modifying the soft and hard building blocks of the polymer.[13,14]

In a study of Baudis et al. (2012), vascular conduits were fabricated from hard-block degradable polyurethane that exhibited satisfactory biomechanical properties as well as good biocompatibility and degradation behavior in a short-term implantation model using rats.[14] These grafts were followed up for 12 months and showed high patency rates and good host cell colonization.[15] For clinical use of TPU, assured graft stability over the period of degradation is required, as bulk degradation of biomaterials leads to deterioration of mechanical properties.[16–18] A biomaterial capable of maintaining its structural integrity during degradation until adequate neo-tissue formation occurs would be a desired solution.

TPUU has been reported to have better mechanical properties compared to TPU.[19] In other studies, these TPUU materials showed good chemical stability but at the same time loss of tensile strength or insufficient hydrolysis, which led to the development of several strategies to overcome these drawbacks.[20–23] However, significant improvement in biomechanical properties could not be achieved. We developed a new TPUU that exhibits self-reinforcing characteristics (patent: WO2022003204A1)[24] after one-week water contact. The design of the TPUU material described in the current study was inspired by Ying et al. (2014), who used dynamic urea bonds to produce reversible and self-healing polyureas.[25]

We hypothesized that the introduction of our modification would result in controlled degradation of the graft without significant loss of biomechanical properties. Blended self-reinforcing TPU/TPUU vascular prostheses were designed (patent: WO2022162166A1).[26] To demonstrate the desired properties, biocompatibility, and hemocompatibility were investigated in vitro. In addition, in vivo performance and graft healing were evaluated in a small animal model.

2. Results

2.1. TPU/TPUU Graft Characteristics and Biomechanical Properties

The grafts described in this study were fabricated from a 50/50 TPU/TPUU blend by electrospinning on a rotating steel mandrel. The self-reinforcing effect was achieved by incorporating hindered urea bonds into the polymer backbone and storage in water for one week after fabrication (**Figure 1**A). The total length of the graft was ≈6 cm. The conduits used for implantation had a length of 2 cm, an inner diameter of 1.6 mm (Figure 1B) and a wall thickness of 130 ± 10 µm. In addition, a dense fiber structure was evident in cross sections of the graft wall (Figure 1C,D). The fibers exhibited a random arrangement (Figure 1E,F). Tensile force (Figure 1G) (dry: 1.04 ± 0.2 N, wet: 2.34 ± 0.3 N) and burst pressure (Figure 1H) (dry: 1625 ± 231 mmHg, wet: 1973 ± 326 mmHg) were significantly increased after water storage, while compliance (Figure 1I) remained unaffected (dry: 7.86 ± 2.04%/100 mmHg, wet: 7.8 ± 1.81%/100 mmHg). Measurements of fiber diameter revealed equal diameters between luminal and adventitial fibers (lumen: 2.59 ± 0.82 µm, adventitia: 2.43 ± 0.67 µm) (Figure 1J).

2.2. In Vitro Biocompatibility

To evaluate the cytocompatibility of TPU/TPUU with cells known to be involved in graft healing and remodeling, human endothelial cells, adipose-derived mesenchymal stem cells (ASCs) and macrophages were seeded on TPU/TPUU and ePTFE controls. **Figure 2**A shows enhanced attachment of endothelial cells on TPU/TPUU compared with ePTFE, as shown by DAPI staining. Moreover, even under static seeding conditions, endothelial cells aligned in a specific direction and exhibited a distinct cytoskeleton on TPU/TPUU (visualized with phalloidin staining, see also Figure S3A, Supporting Information). CD31 was expressed on both polymers mainly in the peri-nuclear region of the cytoplasm, but no significant differences were observed in the expression of CD31 (ePTFE: 284 380.7 ± 57 815.25, TPU/TPUU: 280 274 ± 100 894.68) or phalloidin (ePTFE: 453 546.4 ± 170 721.77, TPU/TPUU: 627 499.1 ± 307 528.86) (Figure 2E). ASCs showed little adhesion on ePTFE and colony-like adhesion on TPU/TPUU. In contrast to endothelial cells, ASC attachment was in general lower on both materials (Figure 2B; Figure S3B, Supporting Information). Interestingly, ePTFE showed lower expression of ASC-specific markers CD73 (ePTFE: 58 872.2 ± 50 768.67, TPU/TPUU: 710 753 ± 427 517.56) and CD90 (ePTFE: 203 176.3 ± 154 428.1, TPU/TPUU: 737 848.1 ± 370 385.87) (Figure 2F). In addition, macrophage adhesion and polarization were analyzed (Figure 2C,D). Again, the cell number was lower on ePTFE compared to TPU/TPUU. The pan-macrophage marker CD68 was significantly less expressed on TPU/TPUU grafts (ePTFE: 297 338.1 ± 101 322.49, TPU/TPUU: 710 753 ± 427 517.56), while low expression of anti-inflammatory CD163 was observed on both materials (ePTFE: 404.4 ± 607.39, TPU/TPUU: 37 573.6 ± 30 599.67). CCR7 was more highly expressed on TPU/TPUU compared to ePTFE (ePTFE: 28 462.7 ± 15 204.12, TPU/TPUU: 150 979.9 ± 98 933.37) (Figure 2G; Figure S3C, Supporting Information).

2.3. In Vitro Hemocompatibility

The thrombogenic potential of TPU/TPUU was tested by evaluating platelet adhesion. Figure S4A (Supporting Information) shows that the number of adherent platelets per ROI was higher on TPU/TPUU than on ePTFE. The result was probably not significant because of high donor variability (ePTFE: 21 ± 9 platelets,

I. Walter
Department of Pathobiology
University of Veterinary Medicine
Veterinaerplatz 1, Vienna 1210, Austria
L. M. Zopf
Ludwig Boltzmann Institute for Traumatology
Donaueschingenstraße 13, Vienna 1200, Austria

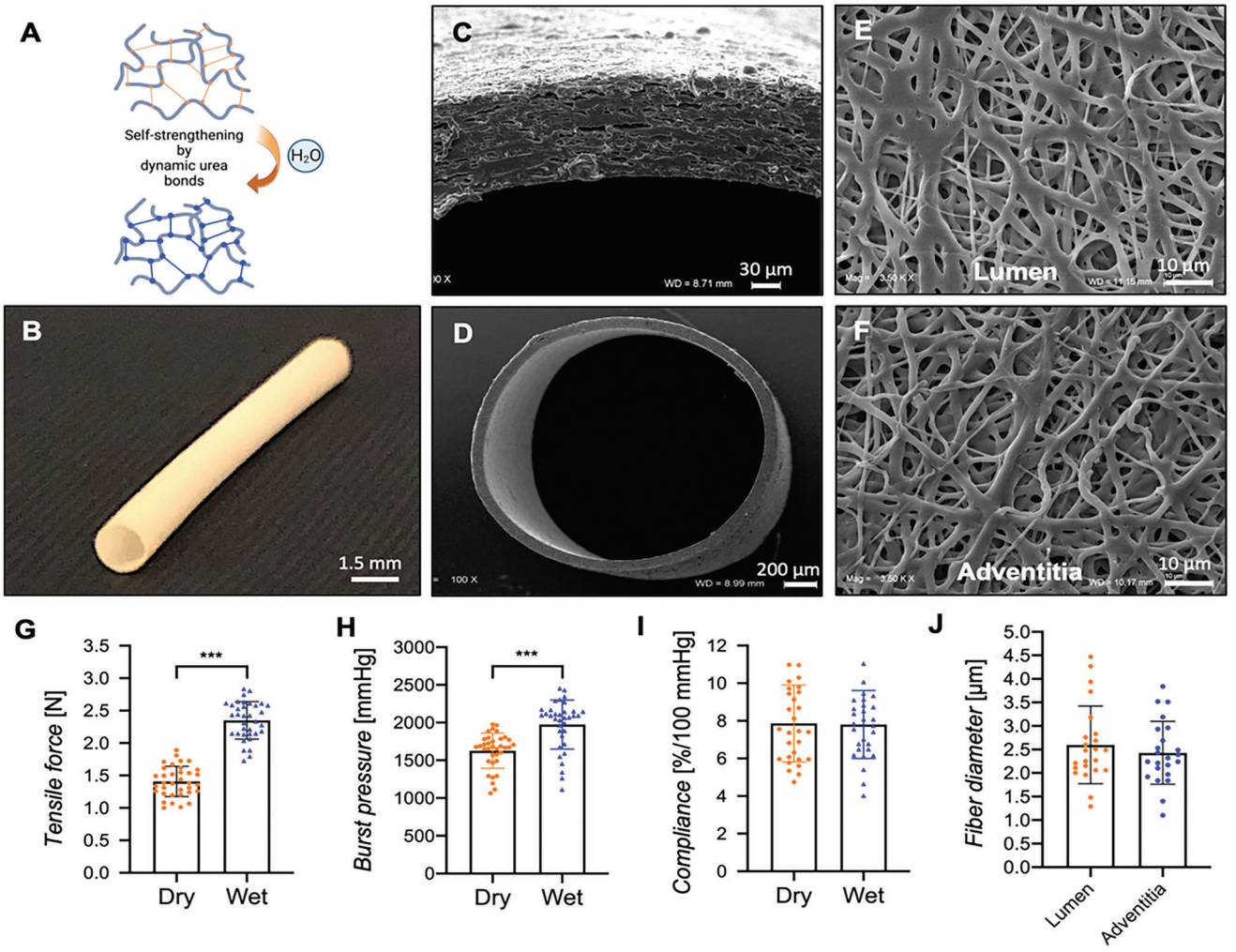

Figure 1. A) Graft properties and biomechanical characteristics of TPU/TPUU grafts. The grafts were fabricated by electrospinning in a high-voltage field. B) The fabricated grafts had a length of 2 cm and an inner diameter of 1.6 mm. C,D) Cross sections of the graft wall showed a dense meshwork of electrospun fibers. E,F) Luminal and adventitial fiber structures were randomly distributed. G) The tensile force and H) burst pressure increased significantly after storage in water ($n = 35$). I) Compliance values remained unchanged ($n = 29$). J) Luminal and adventitial fiber diameters were the same ($n = 29$). Statistical analysis: t-tests, ***: $p \leq 0.001$, mean ± SD.

TPU/TPUU: 26 ± 7 platelets). The results of the hemolysis tests did not show hemolytic properties of TPU/TPUU (Figure S4B, Supporting Information). The hemolysis rate of both materials was in the range of negative control (pos. CTRL: 3.8519%, neg. CTRL: 0.07 ± 0.01%, ePTFE: 0.08 ± 0.24%, TPU/TPUU: 0.04 ± 0.28%).

2.4. In Vivo Performance

TPU/TPUU grafts were implanted in the abdominal aorta of rats and compared with autologous implants. The average length of the TPU/TPUU grafts was 1.5 cm. The length of autologous biopsies was limited to 1 cm. Because of the high elasticity of the aorta, the proximal and distal ends of the native artery retracted after graft harvest. Therefore, it was not possible to perform tension free anastomoses when longer implants were resected. None of the implanted grafts showed signs of chronic inflammation, thrombus formation, or aneurysms. After 3 months, a highly vascularized tissue layer formed on the adventitial side (**Figure 3**A). One animal with TPU/TPUU implant died after 46 days. However, the excised graft was not occluded. Due to the resulting 90% patency of TPU/TPUU implants, the non-inferiority threshold of 15% was met, and the TPU/TPUU conduits were therefore considered patent (Figure 3B). Wall thickness of TPU/TPUU grafts was reduced by 1.6 ± 0.04% at 1 month, 11.6 ± 13.8% after 3 months and 23.7 ± 0.7% after 6 months (Figure 3C). Compliance was significantly reduced after 6 months (0 d: 10.03 ± 0.35, 6 m: 6.45 ± 1.86%/100 mmHg) (Figure 3D). Tensile force (0d: 3.04 ± 0.19 N, 6 m: 3.65 ± 0.51 N) and maximal strain (0 d: 555 ± 4%, 6 m: 539 ± 52%) remained at high levels after 6 months of implantation and did not decrease (Figure 3E,F).

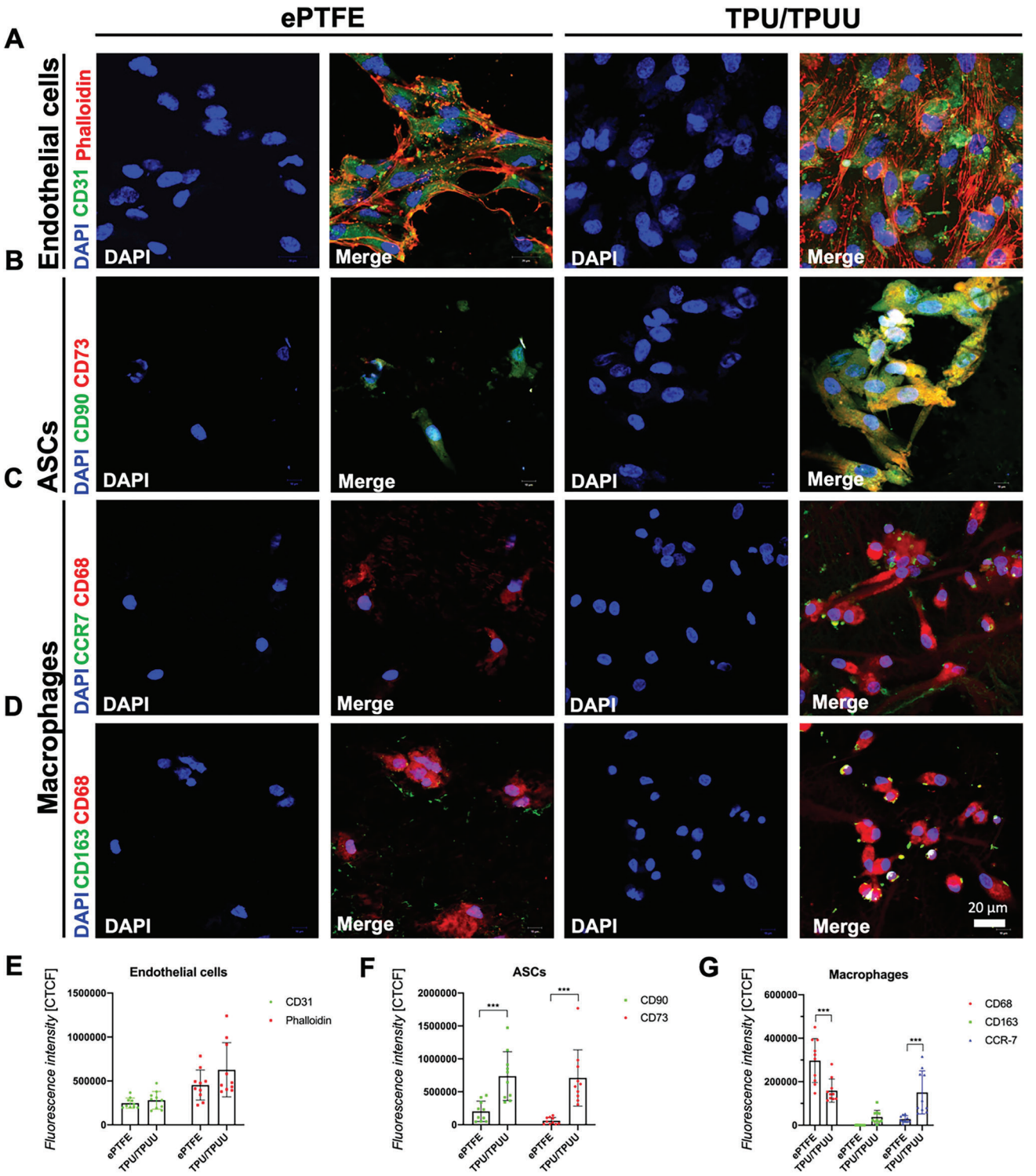

Figure 2. Cell biocompatibility of TPU/TPUU in vitro. A) Endothelial cells showed enhanced attachment and alignment to TPU/TPUU compared to ePTFE. B,F) Increased cell attachment and cell-specific marker expression were also observed for ASCs. C,D) Macrophages did not exhibit a distinct pro- or anti-inflammatory phenotype under either condition but G) quantification of fluorescence signals showed decreased levels of CD68 and increased values for CCR-7 on TPU/TPUU. ($n = 16$). Statistical analysis: Two-way ANOVA, ***: $p \leq 0.001$, mean ± SD.

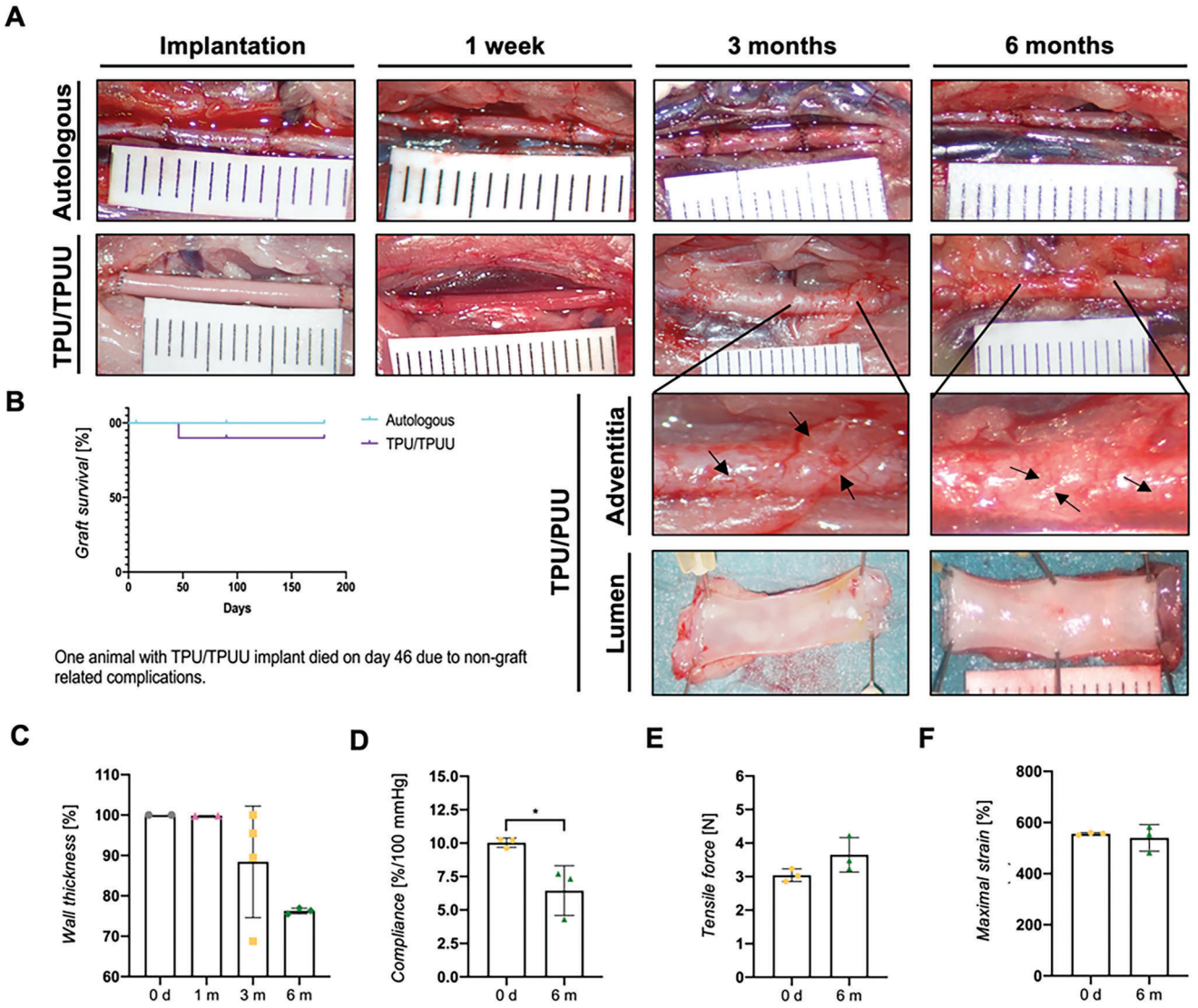

Figure 3. In vivo performance. A) The grafts showed no aneurysmal dilatation, chronic inflammation, or thrombus formation and the newly formed media layer was highly vascularized. B) All grafts remained patent, and only one animal died from complications not related to the grafts. C) Graft wall thickness decreased by 25% after 6 months of implantation ($n = 3$). D) Compliance was significantly reduced after 6 months, E,F) while tensile force and maximal applied strain values remained unchanged ($n = 3$). Statistical analysis: t-test, *: $p \leq 0.05$, mean ± SD.

2.5. Graft Remodeling

Histologic assessment of long-term TPU/TPUU implants (3 months, **Figure 4**A) showed the formation of a neointimal, neomedial, and neoadventitial layer. While the newly formed tissue on the outside of the graft did not have a strong interface with the graft wall, the luminal cell layer appeared to be well fused, as indicated by the H&E staining. The adventitial layer showed only single cell adhesions but no cell infiltration into the graft wall. aSMA-positive cells were detected in the neomedia of TPU/TPUU grafts, but the fluorescence signal was reduced compared with autologous implants (Autologous: 933 154.33 ± 266 282.74, TPU/TPUU: 91 924.43) (Figure S5B, Supporting Information). In addition, the formation of an endothelial layer was demonstrated by vWF staining. μCT analysis confirmed that there was no tissue infiltration from the adventitial side (Figure 4B). Furthermore, polymer degradation was uniform along the entire length of the conduit, and no evidence of bulk degradation or leakage was observed. Moreover, both the luminal and adventitial sides of the graft were covered with cells, as shown by SEM examination (Figure 4B). Closer inspection revealed that the newly formed cell layer around the polymer was not firmly adhered to the TPU/TPUU graft. Instead, the cell layer was easily detached from the polymer material. It was obvious that the dense fiber structure and low porosity prevented cell migration into the graft wall (Figure S5A, Supporting Information). Samples from the mid-graft areas of the implanted conduits were subjected to RT-qPCR analyses to identify inflammatory processes at different time points. Figure 4C shows that the number of macrophages did not change during the implantation

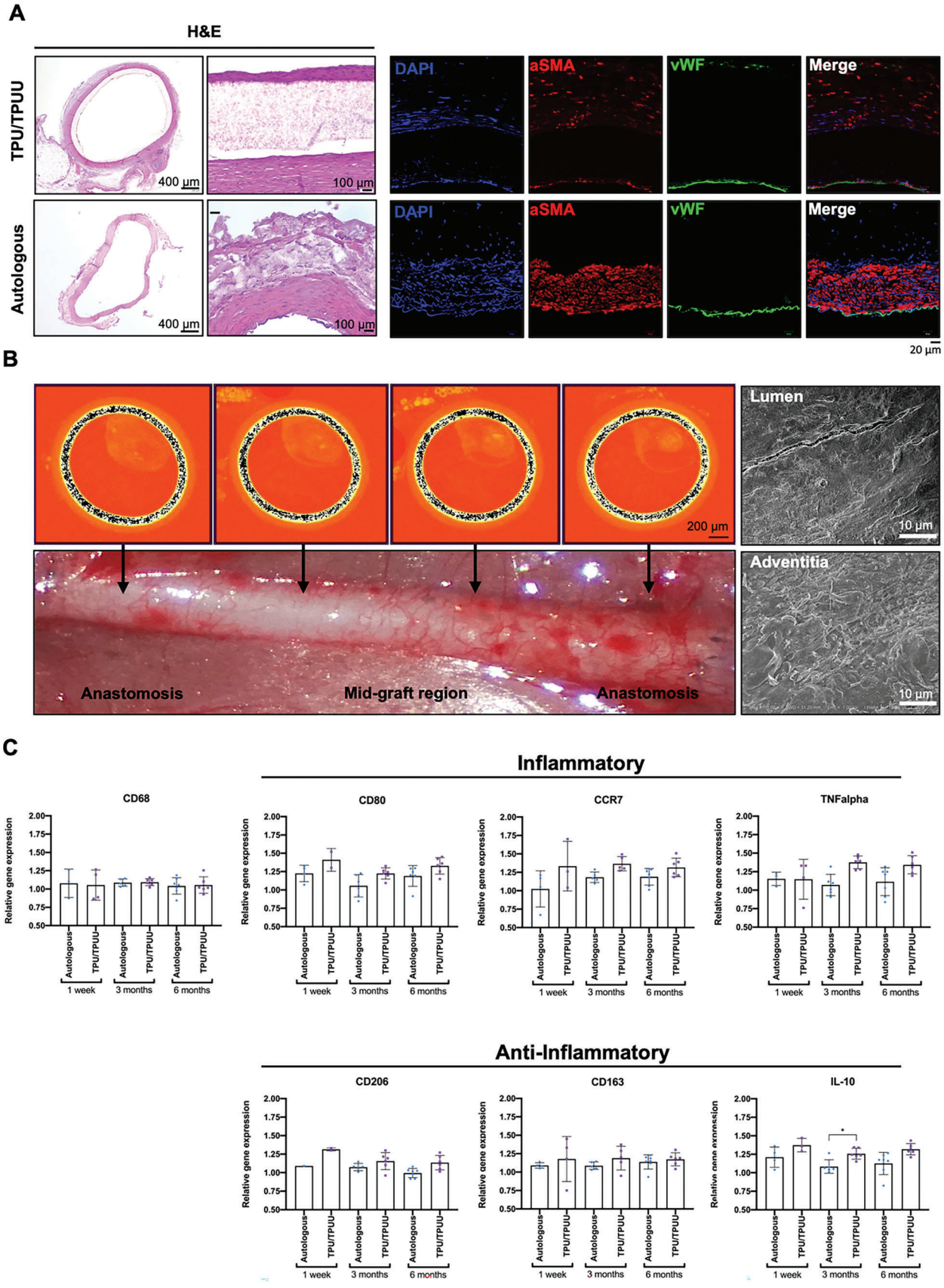

period (CD68 expression). Inflammatory markers CD80, CCR7, and TNFalpha were slightly increased in TPU/TPUU conduits compared with autologous implants, but none of the differences were statistically significant. The anti-inflammatory genes for CD206, CD163, and IL-10 showed a similar expression pattern whereas IL-10 was significantly higher expressed in TPU/TPUU at 3 months (Autologous: 1.08 ± 0.09, TPU/TPUU: 1.26 ± 0.07). Overall, TPU/TPUU did not mediate specific immune responses at any of the observed time points.

2.6. Perivascular Adipose Tissue Signaling

H&E and vWF staining showed that the perivascular adipose tissues (PVATs) that formed around the TPU/TPUU conduits were highly vascularized at 3 months and had vascular structures by 6 months of implantation (Figure S5C, Supporting Information). **Figure 5**A also indicates that the adipocyte markers perilipin 1 (PLIN1), PLIN2, and PLIN3 were expressed. Quantification of fluorescence showed that PLIN1 was significantly increased between 3 months and 6 months of implantation in autologous (3 m: 192 625.3 ± 42 213.63, 6 m: 330 190.65) and TPU/TPUU PVATs (3 m: 156 390.39, 6 m: 439 428.75 ± 135 651.197) and remained significantly higher after 6 months in TPU/TPUU PVATs. PLIN-2 significantly increased in autologous PVATs from 3 to 6 months (3 m: 154 054.86 ± 118 493.08, 6 m: 331 884.45 ± 159 595.831) and was significantly higher in TPU/TPUU PVATs after 3 months (Autologous: 154 054.86 ± 118 493.08, TPU/TPUU: 323 224.05 ± 262 867.39). While PLIN3 was significantly more expressed in TPU/TPUU implants compared with autologous grafts after 3 months (Autologous: 92 822.99 ± 49 464.20, TPU/TPUU: 152 211.57 ± 103 100.03), a significant decrease in expression levels was observed in TPU/TPUU from 3 to 6 months after implantation (3 m: 152 211.57 ± 103 100.03, 6 m: 66 889.93 ± 55 349.61) resulting in a lower expression of PLIN3 in TPU/TPUU compared with autologous PVATs at 6 months (Autologous: 131 919.57 ± 65 762.32, TPU/TPUU: 66 889.93 ± 55 349.61).

In addition, 38 different genes from PVAT involved in biomaterial/host interactions, inflammation, angiogenesis, and remodeling were examined to determine the contribution of PVAT to graft healing (Figure 5B). Gene expression analyses revealed no significant changes between autologous and TPU/TPUU implants for either long-term implantation time point. Therefore, expression changes between 3 months and 6 months were determined separately for PVATs of each graft type. Figure 5C,D shows the genes that were more than 20% differentially regulated in PVATs after 6 months compared with 3 months' implantation. Interleukin (IL)-4 (−24%), IL-1a (−21%), and especially NfκB (−31%) were downregulated in PVATs from autologous implants. TPU/TPUU-PVATs showed a reduction in matrix metalloproteinases (MMP)-9 (−22.48%) and MMP-3 (−22.49%). Interestingly, similar to autologous controls, IL-1a was reduced (−21.87%).

3. Discussion

The current study investigates the performance of a new, self-reinforcing, biodegradable, electrospun polyurethane SDVG. The graft demonstrated excellent biocompatibility and high patency rates in a preclinical study. In addition, the graft was shown to maintain its exceptional biomechanical properties for a period of 6 months after implantation.

As shown in several previous studies, compromised biomechanical properties during degradation of the biomaterial or chronic inflammatory responses can lead to early rupture of the graft.[27,28] Stowell et al. (2020) reported severe inflammation and premature failure of poly(glycerol sebacate)/ poly(ϵ-caprolactone) (PCL) composite conduits in a carotid replacement model in sheep.[27] They hypothesized that the rate of degradation may vary greatly among species and that slower resorption may reduce graft failure caused by the loss of biomechanical strength. Another study showed increased stiffness and chronic inflammation of poly(lactic acid)/PCL grafts when implanted into the arterial circulation of mice and attributed these disadvantages to the choice of polymer composition used.[29]

Due to their good biocompatibility, polyurethanes have been used for the fabrication of vascular grafts in recent years and generally showed satisfying performance in preclinical and clinical studies. Nevertheless, several problems have been reported. Mitrathane, a polyether-urethane-urea graft showed biocompatibility in vitro, but implantation studies as an AV-loop in dogs revealed low patency rates (57% graft failure after 2 months of implantation) due to excessive intimal hyperplasia.[30] Later, a polyester-urethane graft (Vascugraft) performed well in vitro[31,32] and in a rat study[33] but proved unsuitable as a thoracoabdominal bypass in dogs.[34] Despite the drawbacks of the described studies, a recent clinical trial supports the use of TPUs in humans. AVflo grafts showed satisfying secondary patency rates when implanted as hemodialysis access for 2 years.[35,36] As mentioned earlier, the rate of degradation of a biomaterial is critical for its long-term performance in vivo. Depending on the chemical structure of soft and hard segments and the phase separation of TPU(U)s, degradation rates can vary significantly. Polycarbonate urethanes exhibited a 32 ± 9% loss after one year of in vivo implantation, and hard segments were reduced by 21 ± 8%. In contrast, polyether urethanes lost 51 ± 5% of their soft blocks after the same time period and showed a 17 ± 3% degradation of hard segments.[37] The current study used a modification of a previously published hard-block degradable polyurethane that had performed well in implantation studies in rats.[14,15] The material exhibited excellent patency, but remodeling varied among subjects. To allow for more controlled degradation, a dynamic urea group was added into the backbone of the TPU to provide a

Figure 4. In vivo performance. Grafts did not show aneurysms, chronic inflammation, or thrombus formation after 3 months. A) In addition, cells in the adventitial tissue started to express aSMA after 3 months, and endothelial cells (stained by vWF) attached to the lumen. µCT analyses showed uniform degradation of the graft wall along the entire length of the graft. B) SEM images showed cell attachment on the inner and outer surfaces of the grafts after 6 months of implantation. C) Gene expression analyses showed no chronic inflammatory processes during the implantation period. ($n = 7$). Statistical analysis: Two-way ANOVA, *: $p \leq 0.05$, mean ± SD.

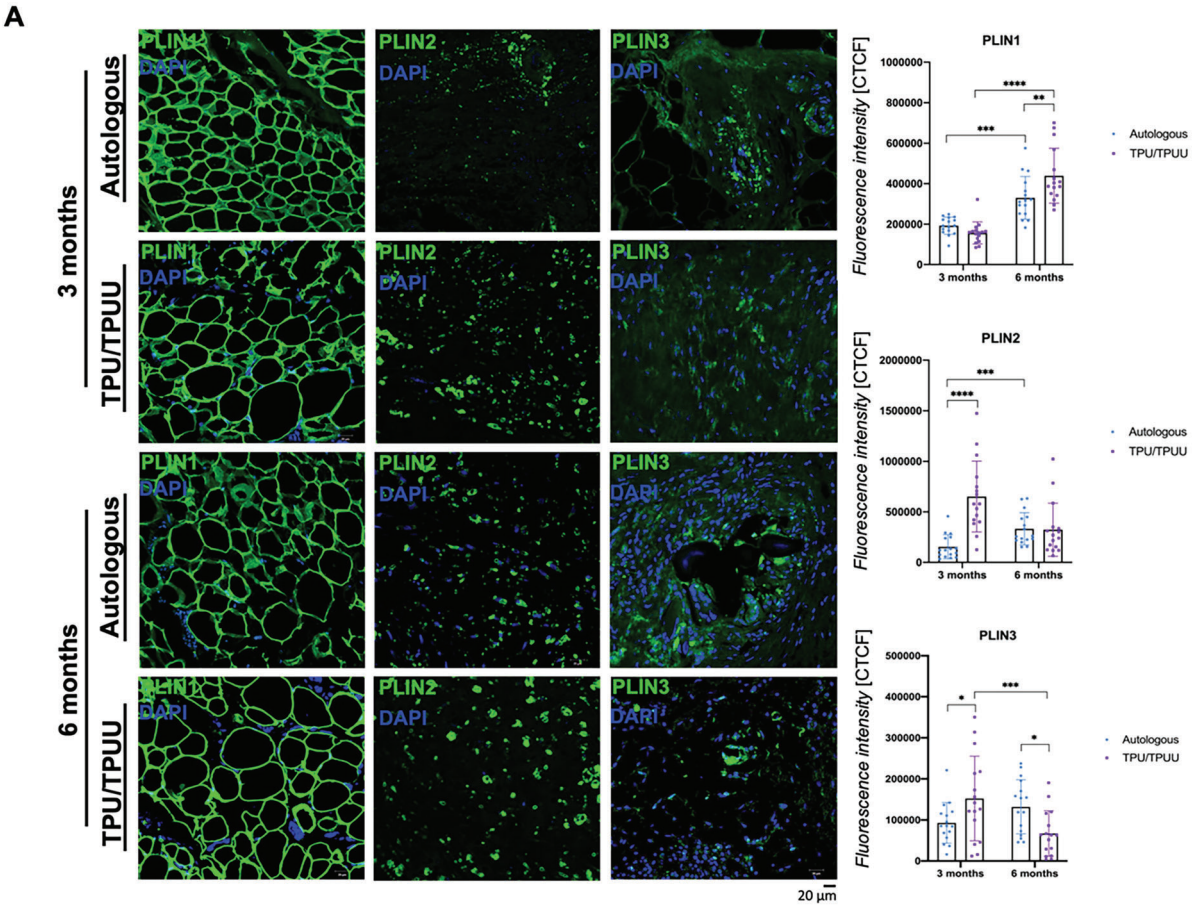

TPUU with self-reinforcing effects upon contact with an aqueous solution.[25]

The material was suitable for the fabrication of thin-walled electrospun grafts with fiber diameters between 1 and 4 μm. A fiber diameter of 0.5 to 1 μm and a pore size in the range of 3–7 μm would be favorable for cell migration.[38] Preliminary studies showed that self-reinforcing TPUU (100%, with no TPU added) could not be processed into grafts with sufficient fiber structure. Therefore, we decided to use a 50:50 mixture of TPUU with a previously published TPU.[14,15] In this way, we were able to produce grafts with excellent biomechanical parameters similar to those of native vessels.[39–43]

Biocompatibility was assessed by seeding of the graft samples with various vessel-specific cells in vitro. HUVECs formed a nearly confluent monolayer on TPU/TPUU after one week, whereas ePTFE showed only sparse attachment of HUVECs. Unmodified ePTFE, as used in the current study, has a patency rate of 39% after 5 years, mainly due to the poor endothelialization and the hydrophobicity of the material.[2,44,45] On both polymers, CD31 expression was observed mainly in the perinuclear region of the cells. This expression pattern was possibly mediated by phosphorylation of the cytoplasmic domain, which is normally observed in endothelial cells located on basal lamina proteins or under flow conditions.[46–48] We hypothesize that the surface structure of the polymers may induce the unfolding of the cytoplasmic domain structure, leading to enhanced mechanosignaling,[48] which would explain the alignment of HUVECs on the relatively rough TPU/TPUU surface without the application of flow. Endothelial cells on ePTFE and TPU/TPUU showed actin filament expression which is important to maintain endothelial functionality in vivo.[49] Mesenchymal stem cells from various sources play important roles in organ function, replacement of dysfunctional cells, cytokine expression[50] and vascular regeneration.[51,52] Because of their high availability and easy isolation, adipose-derived MSCs were used in the present study. CD73 is an important molecule mediating the anti-inflammatory and reparative functions of MSCs[53] and CD90 determines the reprogramming ability of MSCs.[54] Due to the biological importance of these two molecules, their expression on ASCs was investigated. ASCs generally showed lower adhesion to both graft materials than HUVECs. Nevertheless, ASCs expressed significantly higher levels of CD73 and CD90 on TPU/TPUU than on ePTFE. Hollweck et al. (2010) reported low attachment and viability of MSCs and atypical spherical cell morphology on ePTFE,[55] which is consistent with our observations. In one of our previous publications, we showed that macrophages undergo a phenotypic switch from M1 to M2 after 12 weeks of implantation in TPU/TPUU grafts.[56] We therefore tested the expression of phenotypic markers of macrophages seeded on TPU/TPUU and ePTFE. Interestingly, TPU/TPUU inhibited the expression of CD68 and induced polarization into the pro-inflammatory phenotype. It is likely that long-term seeding experiments would provide more insight into marker expression in future studies.

To determine the thrombotic and hemolytic potential of TPU/TPUU before performing the in vivo studies, platelet adhesion and hemolysis assays were performed. We found slightly increased adhesion of platelets to TPU/TPUU compared with ePTFE. Previously, it was described that the size of TPU/TPUU microstructures affects platelet adhesion.[57] Wan et al. (2008) reported that the surface roughness of electrospun materials can strongly affect platelet adhesion. Moreover, polymers can be positively charged after the electrospinning process.[58] Since the surface of platelets is known to be mainly negatively charged,[59] the enhanced adhesion could be due to electrostatic attraction. However, these electrostatic forces could be neutralized by incubating TPU/TPUU in water before the platelet adhesion experiments. Furthermore, neither ePTFE nor TPU/TPUU exhibited hemolytic properties. Another detailed hemocompatibility study of polyurethanes supports our findings by showing that polyurethanes do not exhibit hemolytic potential.[60]

Male Sprague Dawley rats were used to evaluate the biocompatibility and functionality of the grafts in vivo. Autologous controls were selected to compare the synthetic substitutes with the best available substitutes. In our newly designed polyurethanes, aromatic groups were replaced by aliphatic ones to increase the biocompatibility of the synthetic substitutes. The implantation studies confirmed that TPU/TPUU is biocompatible not only in vitro but also in vivo, as evidenced by the absence of inflammation, aneurysm, or thrombus formation. Thus, we demonstrated that the addition of TPUU to TPU does not alter its previously demonstrated excellent biocompatibility and in vivo performance.[14] TPU/TPUU patency rates were equivalent to those of autologous aortic interposition grafts. One animal in the TPU/TPUU group died because of non-graft related complications due to congenital diaphragmatic hernia and pulmonary hypoplasia.

An early study in 1984 showed that polyether urethane grafts failed as AV loops in dogs after only 4 weeks of implantation.[30] Later, Vascugraft, a polyester urethane, showed good results in vitro[31,32] and in a pre-clinical small animal study,[33] but failed as a femoro-popliteal bypass (patency rate: 38 ± 12%) in humans. A major reason for the failure of biodegradable grafts remains chemical and structural instability during polymer degradation. In the current study, we demonstrated that our new TPU/TPUU graft maintained its biomechanical stability 6 months after implantation despite wall thinning caused by degradation. The results therefore represent a breakthrough in enabling controlled degradation of polyether urethane vascular prostheses without significant loss of stability. Previous results have described the failure of polyether urethanes due to chemical instability[16,17] or deformation,[61] and some have even questioned their suitability as medical implants.[37] The addition of a urea group to the TPU macromolecule has been shown to improve its biomechanical

Figure 5. Perivascular adipose tissue signaling. PLIN1 was significantly upregulated in both implantation groups between 3 and 6 months. The expression of PLIN2 was lower than that of PLIN1 but was significantly upregulated in TPU/TPUU at 3 months. A) PLIN3 was downregulated in TPU/TPUU grafts between 3 and 6 months ($n = 16$). B) While some remodeling markers were upregulated in TPU/TPUU after 3 months, gene expression levels of both conditions converged at 6 months ($n = 3$). C) Downregulation of IL-4, IL-1a, and Nfκ-B was observed in autologous implants. D) In TPU/TPUU, in addition to MMP-3 and IL-1a, MMP-9 decreased significantly between 3 and 6 months. Statistical analysis: Two-way ANOVA, ****: $p \leq 0.0001$, ***: $p \leq 0.001$, **: $p \leq 0.01$, *: *: $p \leq 0.05$, mean ± SD.

properties.[21] However, other studies reported that the incorporation of dynamic urea bonds results in deterioration of the mechanical characteristics during self-healing and rapid degradation of the materials.[24,62] In the current study, we demonstrated that our TPU/TPUU has overcome these drawbacks. Mechanical testing in the current study showed that the burst and elongation strength remained unchanged despite a significant reduction in the size of the graft wall. Self-reinforcement during implantation and the formation of a tissue layer on the adventitial side of the graft may have been the reasons for a decrease in compliance after 6 months. However, TPU/TPUU compliance was still at values close to the coronary artery range (8–17%/100 mmHg).[43]

After 1 week, no difference from freshly implanted grafts could be seen, as no tissue formed outside the graft. Neomedia was visible 3 months after implantation and matured after 6 months. After 3 months, aSMA-positive cells were detected in the newly formed tissue indicating the formation of contractile smooth muscle tissue[63] around the graft. Both autologous and TPU/TPUU implants exhibited an endothelial lining in the lumen. The neomedia was surrounded by newly formed and highly vascularized perivascular adipose tissue. μCT analyses showed that no remodeling by cell infiltration occurred throughout the graft. Instead, the material was degraded by surface erosion. We hypothesize that the differences in the fiber structure of the modified TPU/TPUU did not allow cell infiltration despite the chemical similarities with TPU. Remodeling of the grafts was similar to our previously designed polycarbonate urethane vascular grafts, which showed good vascularization of the newly synthesized tissue after one year of implantation despite presence of residual polymeric material.[64] We therefore expect similar results for TPU/TPUU in longer implantation studies. Surface patterns resembling the natural extra-cellular matrix structure on a scale of nanometers to micrometers showed higher endothelialization rates than random topographies,[65] which are prevalent in the examined grafts and may explain the longer endothelialization times needed.

Gene expression analyses showed no contribution of pro- or anti-inflammatory mediators during the degradation process. To gain a better understanding of the mechanisms leading to neomedia formation, detailed analyses of PVATs from 3- and 6-month implants were performed. We hypothesized that PVAT may have an impact on tissue formation as it is an important mediator of vascular hemostasis by secreting vasoprotective factors and targeting smooth muscle cells.[66] First, the expression of different lipid droplet proteins (PLIN1, PLIN2, PLIN3) was observed. PLIN1 is a protein located on the surface of lipid droplets and is expressed exclusively on adipocytes and steroidogenic cells.[67–69] Zou et al. (2016) showed that PLIN1-null mice exhibited dysregulation of PVAT, developed spontaneous hypertension, and had high expression of inflammatory markers.[69] Therefore, the increase in PLIN1 expression in both types of grafts during the implantation period suggests the formation of a functional PVAT. In contrast, PLIN2 has been shown to be expressed on metabolically activated macrophages (MMe) and to serve as a pro-inflammatory marker.[70,71] The upregulation of PLIN2 in TPU/TPUU-PVATs after 3 months indicated some inflammatory response and infiltration of MMes from the surrounding adipose tissue. However, this response attenuated after 6 months to the same levels observed in PVATs from autologous implants. Similar to PLIN2, PLIN3 expression is not restricted to adipocytes.[72] PLIN3 has been shown to restrict lipid metabolism and thermogenic gene expression, thereby inhibiting the formation of disproportionate amounts of brown fat.[73] The changes in expression levels observed in the current study suggest that newly formed PVATs regulate their composition to maintain functional integrity.

The results of gene expression analyses showed no significant differences between autologous and TPU/TPUU implants. Interestingly, the expression of several genes in the PVAT decreased over time. In autologous implants, the expression of IL-4, a stimulator of extra-cellular matrix deposition, remodeling, and vascular stabilization,[74] decreased. Most likely, the surgical procedure, particularly dissection of the aorta followed by removal of PVAT, led to proliferation of IL-4 stimulated M2a macrophages that rebuild the tissue. The decrease in nuclear factor "kappa-light-chain-enhancer" of activated B-cells (NfκB) in autologous implants has been associated with improved vascular homeostasis, as increased NfκB levels are usually associated with intimal hyperplasia and atherosclerotic plaque formation.[75] In addition, a decrease in IL-1a has been observed in both autologous and TPU/TPUU implants. Stimulation of IL-1a promotes stromal-derived factor-1 (SDF-1) in vascular smooth muscle cells, leading to increased remodeling of vascular implants.[76] The decrease in MMP-9 in TPU/TPUU implants is related to the decrease in MMP-3, as MMP-3 activates MMP-9 driven SMC migration.[77] Moreover, MMP-3 together with MMP-1 has been shown to stimulate the expression of MMP-9 in macrophages, leading to inflammation, wound healing, and tissue formation.[78] In conclusion, gene expression data from PVATs suggest that remodeling processes slowed down from 3 to 6 months of implantation, with no evidence of chronic inflammation.

4. Conclusion

The results of the current study represent a breakthrough in demonstrating controlled in vivo degradation of polyether urethane vascular prostheses without significant loss of biomechanical stability. The grafts exhibited excellent biocompatibility and biomechanical properties both in vitro and in vivo. TPU/TPUU could therefore be the next step toward a biodegradable tissue-based vascular graft for challenging clinical applications.

5. Limitations

TPU/TPUU vascular prostheses exhibit favorable properties for clinical use as SDVG. Degradation was slow but uniform along the entire graft length, with no evidence of aneurysm formation after 6 months. Because vascular prostheses must withstand arterial pressure, aneurysm formation could occur after complete graft degradation and inadequate tissue regeneration. However, the formed neomedia/neoadventitia represents a differentiated vascular tissue capable of meeting the hemodynamic requirements of arterial vascular structures. We have shown in previous studies that the biomechanical requirements are met after long-term application of one of the polymer blends alone (TPU) and

that the remodeled grafts exhibited similar biomechanical properties as native blood vessels.[15]

However, longer implantation periods would be beneficial to gain more insight into the long-term degradation behavior of TPU/TPUU and graft remodeling. Modifications of the graft wall should be further considered for future applications to promote increased cell migration.

6. Experimental Section

Polymer Synthesis: Standard Schlenk-techniques were used for the synthesis of both polymers. The structural formulas for both, TPU and TPUU, are shown in Figure S2A (Supporting Information).

For the synthesis of TPU, dry poly(tetrahydrofuran) (pTHF, $\bar{M}_w$ = 1000g mol^{-1}, Sigma Aldrich, 37 ppm H_2O, 5.121 g, 5.0 mmol, 1.0 eq) was weighed directly into the reaction flask and dried in vacuo at 60 °C for an hour. Hexamethylene diisocyanate (HMDI, Fluka, 1.174 g, 10.0 mmol, 2.0 eq) was added to the reaction vessel, and the transfer syringe and vessel were rinsed with dry dimethylformamide (DMF, Sigma Aldrich, 10 mL) in portions. Three drops of stannous octoate ($Sn(Oct)_2$, Sigma-Aldrich, USA, 150 µL) were added to the reaction mixture. After stirring at 60 °C for 3.5 h, bis(2-hydroxyethylene) terephthalate (BHET, recrystallized, Sigma Aldrich, 1.304 g, 5 mmol, 1 eq) was dissolved in dry DMF (5 mL) and added to the reaction mixture, followed by the same rinsing procedure as for HMDI. Stirring was continued overnight at 60 °C. The resulting highly viscous mixture was diluted with DMF (70 mL) and the polymer was precipitated in methanol (1.5 L) and filtered. After drying, TPU (6.6 g, 87%) was obtained. The molecular weight was determined by gel permeation chromatography (GPC) (conventional calibration with PS-standards).

SEC: $\bar{M}_w$, = 90 kDa, Đ= 1.7

^{1}H-NMR (200 MHz, $CDCl_3$): δ [ppm] = 8.09 (4H, H^{ar}), 4.92 (2H, NH), 4.673 (2H, NH), 4.49 (4H, $CH_2C(=O)O$), 4.39 (4H, OCH_2), 4.04 (5H, OCH–), 3.40 (55H, CH_2), 3.13 (8H, CH_2), 1.60 (55H, CH_2), 1.46 (8H, CH_2), 1.31 (8H, CH_2).

ATR-IR = 3325 cm^{-1} ν(N-H···N-H, urethane), 2914 cm$_{-1}$ ν(C–H), 2850 cm^{-1} ν(OC–H), 1718 cm^{-1} ν(C=O, ester), 1688 cm$_{-1}$ ν(C=O···H-N, urethane, ordered), 1540 cm^{-1} δ(NH, urethane) + ν(C–N, urethane), 1258 cm^{-1} ν(C–O, ether), 1100 m^{-1} ν(C–C).

For the synthesis of TPUU (PCT/EP2021/06 8506), pre-dried pTHF (19 ppm H_2O, 6.059 g, 6.10 mmol, 1.00 eq.) was weighed into the reaction flask and dried for 1 h at 60 °C. To the dry molten polymer, dry DMF (5 mL) and HMDI (2.111 g, 12.20 mmol, 2.00 eq.) were added. The syringe and transfer vessel were rinsed with dry DMF (5 mL). Two drops of $Sn(Oct)_2$ were added, and the reaction was stirred at 60 °C under argon. After 3 h, BHET, (0.5 eq. 2.8 mmol, 0.7062 g) was dissolved in dry DMF (10 mL) and added to the reaction mixture. Both, the transfer tube and syringe were rinsed with dry DMF (10 mL), and stirring was continued at 60 °C. After 3 h, the heating was turned off and after the mixture cooled to room temperature, di(*tert*-butyl)ethylenediamine (Fluka, 0.478 g, 2.8 mmol, 0.5 eq) was added. Again, the syringe was rinsed with dry DMF (10 mL). Shortly thereafter, white flocs formed in the reaction mixture. The viscosity of the reaction mixture increased rapidly, so more volume of dry DMF (20 mL) was added. Stirring at room temperature was continued overnight. To precipitate the polymer, the viscous solution was diluted with DMF and added dropwise to diethyl ether (1 L). The white precipitate formed immediately and was filtered off and air dried for 3 days. The structure of the polymer was confirmed by GPC and nuclear magnetic resonance imaging.

$\bar{M}_w$ = 65.570, Đ = 2.1

^{1}H-NMR (400 MHz, $CDCl_3$): δ [ppm] = 8.11 (4H, H^{ar}), 4.90 (4H, NHC(=O)N), 4.71 (5H, NHC(=O)O), 4.52 (4H, $CH_2CO(=O)$), 4.41 (4H, OCH_2), 4.06 (9H, OCH_2), 3.41 (94H, OCH_2), 3.26 – 3.05 (16H, CH_2), 1.62 (110H, CH_2), 1.53 – 1.15 (51H, NCH_2, CH_2, $NC(CH_3)_2$).

ATR-IR = 3320 cm^{-1} ν(N–H···N–H, urethane), 2935 cm^{-1} ν(C–H), 2850 cm^{-1} ν(OC–H), 2795 cm^{-1} ν(N–CH2), 1715 cm^{-1} ν(C=O, ester; C=O···H–N, urethane, unordered), 1682 cm^{-1} ν(C=O···H–N, urethane, ordered), 1670 cm^{-1} ν(C=O···H–N, urea, unordered), 1630 cm^{-1} ν(C=O···H–N, urea, ordered), 1540 cm^{-1} δ(NH, urethane) + ν(C–N, urethane), 1258 cm^{-1} ν(C–O, ether), 1100 cm^{-1} ν(C–C).

Electrospinning: Preliminary tests showed that a polymer mix of 50/50 (TPU/TPUU) had advantageous effects on pore size as well as mechanical properties compared to other blend ratios (Figure S2B, Supporting Information). Therefore, this ratio was chosen for all further experiments. The polymer blend was dissolved in hexafluoro-2-propanol (Sigma-Aldrich, USA). The nanofibrous conduits were fabricated using a custom electrospinning device that included a high-voltage generator, a syringe pump, a syringe with a 21 G blunt-ended needle, a Ø1.6 mm Teflon mandrel and an auxiliary electrode. The flow rate of the polymeric solution was set at 0.7 mL h^{-1} and charged at 8.5 kV. The potentials of the rotating mandrel and auxiliary electrode were adjusted to achieve an optimal fiber deposition rate. The complete electrospinning device was placed in a Faraday cage and operated in a class 1000 clean room at 24 °C and a relative humidity of 34%. The obtained electrospun grafts were cut into 20 mm wide pieces and stored in water at room temperature for 7 days. After drying, sterilization of the grafts was facilitated by ethylene oxide.

Biomechanical Testing: Biomechanical properties were evaluated as previously described[79] on water-stored and dry-stored graft specimens with 5% polymer concentration. Briefly, a uniaxial BOSE Electroforce LM1 test bench system (TA Instruments, New Castle, USA) was used to perform hoop-tensile tests. Graft rings of 2 mm length were placed on two aligned steel pins of 0.6 mm diameter and loaded to failure at a crosshead speed of 10 mm min^{-1}. The compliance (% diameter change/100 mmHg) was determined over the pressure range of 80–120 mmHg. In addition, the burst pressure was determined using Laplace's law. Grafts stored in water with a polymer concentration of 8% were used for all subsequent experiments.

Scanning Electron Microscopy (SEM): Graft specimens were placed on specimen holders either as cross sections or with the luminal or adventitial side up. Implanted samples were fixed in glutaraldehyde (Sigma-Aldrich, USA, 2.5%) and then dehydrated with an increasing ethanol series, followed by a final dehydration step in hexamethyldisilazane (HMDS, Sigma-Aldrich, USA). Samples were sputter coated with 20 nm gold and analyzed using a Zeiss EVO 10 microscope (Zeiss, Austria).

Cell Culture: Cells were incubated under standard cell culture conditions at 37 °C, in 5% CO_2 and 95% humidity. Human umbilical vein endothelial cells (HUVECs) were purchased as a pooled donor batch (Lonza, Switzerland). Adipose-derived mesenchymal stem cells (ASCs) were kindly provided by Wolfgang Holnthoner from the Ludwig Boltzmann Institute for Traumatology (Vienna, Austria). Endothelial progenitor cells (EPCs) were isolated as previously described.[80] In brief, freshly donated blood from healthy male and female donors (45 mL) was collected by venipuncture into sodium citrate tubes (Vacuette, Greiner Bio-One, Austria) after informed consent and approval by the local ethics committee of the Medical University of Vienna (EK nr. 2321/2020). Peripheral blood mononuclear cells (PBMCs) were isolated after a 30-min density centrifugation using Ficoll Paque Plus (GE Healthcare, Austria). The recovered cells were washed twice with PBS by centrifugation at 300 x g for 10 min. HUVECs, ASCs, and EPCs were all cultured in Endothelial Growth Medium-2 (EGM-2, Lonza, Switzerland) supplemented with additional fetal bovine serum (FBS, Thermo Fisher, USA, 10%) and penicillin/streptomycin (Pen Strep, Gibco, USA, 1%). Monocytes were isolated according to the same protocol as EPCs but cultured in Roswell Park Memorial Institute (RPMI) medium (Sigma-Aldrich, USA) supplemented with GlutaMAX, FBS (10%) and 2-mercaptoethanol (0.05 mM) (Thermo Fisher, USA). Three hours after isolation, a first medium change was made and RPMI with macrophage colony stimulating factor (M-CSF, Biolegend, USA, 50 ng mL^{-1}) was added. Another medium change was made after 3 days (again with M-CSF). Mature macrophages were used for experiments four days after isolation.

In Vitro Biocompatibility: To evaluate the biocompatibility of TPU/TPUU grafts, HUVECs, ASCs, EPCs, and undifferentiated macrophages were seeded onto the graft samples. Aeos^{TM} ePTFE grafts (Zeus Industrial Products, USA) were used as control material. The grafts were cut into 6 × 3 mm specimens and inserted into 96

well plates (Sigma-Aldrich, USA). The specimens were seeded with 1×10^4 cells of each cell type and incubated for one week under standard cell culture conditions. Subsequently, the samples were washed three times with 1 x phosphate buffer saline (PBS) and fixed overnight at 4 °C in paraformaldehyde (PFA, 4%). Samples were washed again in PBS and removed from well plates.

Immunofluorescence staining was performed to determine cell-type specific marker expression and morphology of seeded cells as previously described.[78] Samples were washed twice with PBS and nonspecific binding of antibodies was blocked with PBS/1%BSA for 1 h. Mouse anti-human CD31-Fluoresceinisothiocyanate (FITC, BD Biosciences, USA) and phalloidin iFlour-555 reagent (Abcam, USA) were used for staining HUVECs. ASCs were stained with mouse anti-human CD73-Phycoerythrin (PE) and mouse anti-human CD90-FITC (both from Miltenyi Biotec, Germany). Mouse anti-human CD68, rabbit anti-human CCR-7 and rabbit anti-human CD163 (all from Abcam, USA) were used to detect pan-, anti-, and pro-inflammatory proteins on macrophages. All primary antibodies were incubated at room temperature for 40 min. If necessary, samples were washed three times and further incubated with secondary antibodies goat anti-mouse 647 or goat anti-rabbit 488 (both Abcam, USA). Samples were embedded on slides with fluorescence mounting medium (Dako, USA) containing 4',6-diamidino-2-phenylindole-dihydrochloride (DAPI, Sigma-Aldrich, USA, 1 µM) and imaged with an LSM700 confocal microscope (Zeiss, Germany).

Hemocompatibility Assessments: Platelet adhesion was observed to evaluate the thrombogenicity of TPU/TPUU compared with ePTFE grafts. Blood collection was performed as described above. After centrifugation with Ficoll Paque Plus, the top layer was transferred to a new 50 mL Falcon tube and topped up to 50 mL with PBS before another centrifugation step at 300 x g for 10 min. The platelet-rich plasma (upper 2/3 of the solution in the Falcon tube) was incubated with 6 × 3 mm graft samples at 37 °C for 2 h. Samples were then fixed overnight at 4 °C in glutaraldehyde (2.5%) and dehydrated for SEM analysis with increasing ethanol series and a final HMDS step.

The hemolytic potential of TPU/TPUU was determined by incubating the graft samples with 1:5 diluted blood containing NaCl (0.9%) at 37 °C for 1 h. A positive control was performed with distilled water instead of NaCl, whereas a dilution with NaCl but no sample served as a negative control. After the incubation period, samples were centrifuged at 300 x g for 5 min and the supernatant was subjected to absorbance measurement at 541 nm. The following formula was used to calculate the hemolysis rate: *((Absorbance[samp]-Absorbance[neg])/(Absorbance[pos]-Absorbance[neg])) *100%*

Animal Model: The animal experiments were approved by the institutional Ethics Committee and authorized by the Federal Ministry of Science and Research (GZ: BMWFW-66.009/368-V/3b/2019, Helga Bergmeister). All animals were treated in accordance with the principles of Good Scientific Practice Guidelines of the Medical University of Vienna. Anesthetic and analgesic procedures were performed as previously described.[79] Electrospun TPU/TPUU grafts (length: 2 cm, inner diameter: 1.6 mm) and autologous aortic grafts were implanted in male Sprague Dawley rats (450–590 g) for 7 days, 3 months and 6 months (each time point $n = 7$). The grafts were inserted into the infrarenal host aorta using a surgical microscope (Zeiss Vario S88, Zeiss, Austria). End-to-end anastomoses were performed with non-absorbable sutures (Monosof 10/0, Covidien, USA). Before implantation, the conduits were flushed with physiological saline containing heparin (5 IU mL^{-1}). No anti-coagulation or anti-platelet medications were administered during or after the study. At harvest, the grafts were cut into samples for SEM, histology, and gene expression analyses.

Magnetic Resonance Imaging (MRI) and Micro-Computed Tomography (µCT): µCT was performed to determine the degradation of the graft wall in a whole explanted graft after 6 months of implantation. The graft was fixed in PFA (4%) for 24 h and then stained in 15 mL Lugol's solution (1/3 iodinine, 2/3 potassium iodide in aqueous solution, both Sigma-Aldrich, USA, 0.5%, 15 mL). To achieve a concentration of 0.5%, potassium iodide was dissolved in double-distilled water. The µCT scans were performed using a SCANCO µCT 50 (SCANCO Medical AG, Switzerland) specimen µCT scanner. A high-resolution scan was performed with 70 kVp (57 µA, 0.5 mm Al filter, 1000 projections, 740 ms integration time) with an isotropic resolution of 3.4 µm. The LUTs plugin in ImageJ was used to create pseudocolored images of the µCT measurements to better visualize the degradation of the vessel wall.

Histology: Histological evaluation of explanted grafts was similar to previous studies.[64,81] Grafts were fixed in buffered PFA (4%) for 24 h and then stored in ethanol (70%) until further processing. Tissues were then dehydrated with an ascending ethanol series and embedded in paraffin using a TissueTek VIP 6 automated embedding device (Sakura Finetek, USA). For general morphological observation, 3 µm tissue sections were stained with Hematoxylin and Eosin (H&E). In addition, immunohistochemical examination was performed for endothelialization and formation of the medial/adventitial layer. Samples were blocked with normal goat serum (Sigma-Aldrich, USA, 10%) for 60 min at room temperature. Specimens were incubated with primary antibodies overnight at 4 °C. Endothelial cells were labeled with rabbit anti-von Willebrand factor (vWF) and smooth muscle cells (SMCs) were stained with mouse anti-smooth muscle actin (SMA) (both from Agilent, USA). PVAT was stained with rabbit anti-PLIN1 (Abcam, USA), mouse anti-PLIN2 (AntikörperOnline, Germany) and PLIN3 (Santa Cruz, USA). Staining of vWF and PLIN1 was performed with a secondary poly-HRP-anti-rabbit antibody, whereas SMA, PLIN2, and PLIN3 were visualized in a second step by addition of poly-HRP-anti-mouse (both from Immunologic, Netherlands). Detection was performed by adding fluorescently labeled Tyramid solutions in Tris-HCl pH 7.4 (Sigma-Aldrich, USA) for 10 min. Samples were counterstained with DAPI (Sigma-Aldrich, USA) and embedded in Mowiol (Sigma-Aldrich, USA) or AquaPolymount (Fisher Scientific, USA) mounting medium.

Gene Expression Analysis: The graft samples were stored in RNA later solution (Thermo Fisher, USA) until processing. RNA was isolated using a FavorPrep™ Tissue Total RNA Purification Mini Kit (Favorgen, Austria) according to the manufacturer's instructions. RNA quantity and quality was assessed using a SPARK microplate reader (Tecan, Austria). Reverse transcription into cDNA was performed using a reverse transcription kit (Qiagen, Germany) according to the manufacturer's instructions. cDNA (30 ng) was used together with SYBR Green PCR Master Mix (Applied Biosystems, USA) and the appropriate primers (10 µM, see Figure S1, Supporting Information) for each reaction. RT-qPCR was performed using a 7500 Fast Real-Time PCR system (Applied Biosystems, USA).

Statistical Analysis: All in vitro experiments were performed with at least three biological replicates. Cells were either isolated from different donors or, in the case of purchased cells, used as pooled donor batches in different passages to increase power. In vitro experiments were designed and performed as balanced designs. Statistical analyses were performed using Prism 6 software (GraphPad, USA). Normality of distribution was tested using a D'Agostino's K-squared test. In case of normality, t-tests were performed. Mann-Whitney-U tests were performed if the measurements did not show a normal distribution. To analyze differences between time points and conditions, 2-factorial analysis of variance (ANOVA) was performed. p-values < 0.05 were considered significant. Data were presented as mean ± SD. Significances were represented as asterisks (****: $p \leq 0.0001$, ***: $p \leq 0.001$, **: $p \leq 0.01$, *: $p \leq 0.05$).

Because it was assumed that the autologous control group would perform similarly to the intact native aorta, the in vivo portion of the study was designed as noninferiority active-controlled study. The noninferiority margin was set at 15% because of the unpredictable biological performance of TPU/TPUU and the experience in the field of SDVG development. Performance was assessed by time and described exploratively. Qualitative assessments of endothelialization and intimal hyperplasia were also performed. Statistical analyses of biomechanical properties, gene expression and fluorescence quantification after implantation were performed as described for the in vitro part.

Supporting Information

Supporting Information is available from the Wiley Online Library or from the author.

Acknowledgements

The authors would like to thank the team of the Medical University of Vienna Imaging Core Facility for the imaging support, especially beloved colleague Marion Gröger who sadly passed away in 2022. Moreover, the authors highly appreciate the work of Claudia Höchsmann who performed the histological processing of the in vivo samples and Patrick Heimel for his support regarding µCT images. The authors further thank Wolfgang Holnthoner from the Ludwig Boltzmann Institute for Traumatology (Vienna) for providing the ASCs.

Conflict of Interest

H.B., B.K.P., H.S., C.G., S.B., R.L., K.E., and S.R. have a patent PCT/EP2022/052088 pending and licensed to BioDGraft, an academic spin-off company aiming to develop biodegradable vascular grafts. S.B., R.L., K.E. have a patent PCT/EP2021/068506 pending and licensed to BioDGraft. H.B., H.S., C.G. have a patent PCT/EP2021/08682 pending and licensed to BioDGraft. BioDGraft has neither funded the current study nor influenced the conduct, description or interpretation of the findings in this report.

Data Availability Statement

The data that support the findings of this study are available from the corresponding author upon reasonable request.

Keywords

biodegradables, self-reinforcing, small diameter vascular grafts, tissue engineering

Received: February 17, 2023
Revised: April 21, 2023
Published online:

[1] P. Mallis, A. Kostakis, C. Stavropoulos-Giokas, E. Michalopoulos, *Bioengineering* **2020**, *7*, 160.
[2] F. O. Obiweluozor, G. A. Emechebe, D. Kim, H. J. Cho, C. H. Park, C. S. Kim, I. S. Jeong, *Cardiovasc. Eng. Technol.* **2020**, *11*, 495.
[3] M. Carrabba, P. Madeddu, *Front. Bioeng. Biotechnol.* **2018**, *6*, 41.
[4] M. A. Cleary, E. Geiger, C. Grady, C. Best, Y. Naito, C. Breuer, *Trends Mol. Med.* **2012**, *18*, 394.
[5] E. Benrashid, C. C. McCoy, L. M. Youngwirth, J. Kim, R. J. Manson, J. C. Otto, J. H. Lawson, *Methods* **2016**, *99*, 13.
[6] T. Shin'oka, Y. Imai, Y. Ikada, *N. Engl. J. Med.* **2001**, *344*, 532.
[7] W. Wystrychowski, L. Cierpka, K. Zagalski, S. Garrido, N. Dusserre, S. Radochonski, T. N. McAllister, N. L'Heureux, *J. Vasc. Access* **2011**, *12*, 67.
[8] S. L. Dahl, A. P. Kypson, J. H. Lawson, J. L. Blum, J. T. Strader, Y. Li, R. J. Manson, W. E. Tente, L. DiBernardo, M. T. Hensley, R. Carter, T. P. Williams, H. L. Prichard, M. S. Dey, K. G. Begelman, L. E. Niklason, *Sci. Transl. Med.* **2011**, *3*, 68.
[9] R. D. Kirkton, M. Santiago-Maysonet, J. H. Lawson, W. E. Tente, S. L. M. Dahl, L. E. Niklason, H. L. Prichard, *Sci. Transl. Med.* **2019**, *11*, 485.
[10] P. D. Ballyk, C. Walsh, J. Butany, M. Ojha, *J. Biomech.* **1998**, *31*, 229.
[11] W. M. Abbott, J. Megerman, J. E. Hasson, G. L'Italien, D. F. Warnock, *J. Vasc. Surg.* **1987**, *5*, 376.
[12] K. Hayashi, K. Takamizawa, T. Saito, K. Kira, K. Hiramatsu, K. Kondo, *J. Biomed. Mater. Res.* **1989**, *23*, 1247.
[13] R. J. Zdrahala, *J. Biomater. Appl.* **1996**, *11*, 37.
[14] S. Baudis, S. C. Ligon, K. Seidler, G. Weigel, C. Grasl, H. Bergmeister, H. Schima, R. Liska, *J. Polym. Sci., Part A: Polym. Chem.* **2012**, *50*, 1272.
[15] H. Bergmeister, N. Seyidova, C. Schreiber, M. Strobl, C. Grasl, I. Walter, B. Messner, S. Baudis, S. Frohlich, M. Marchetti-Deschmann, M. Griesser, M. di Franco, M. Krssak, R. Liska, H. Schima, *Acta Biomater.* **2015**, *11*, 104.
[16] R. R. Joshi, T. Underwood, J. R. Frautschi, R. E. Phillips, F. J. Schoen, R. J. Levy, *J. Biomed. Mater. Res.* **1996**, *31*, 201.
[17] K. Stokes, A. Coury, P. Urbanski, *J. Biomater. Appl.* **1987**, *1*, 411.
[18] K. Ehrmann, P. Potzmann, C. Dworak, H. Bergmeister, M. Eilenberg, C. Grasl, T. Koch, H. Schima, R. Liska, S. Baudis, *Biomacromolecules* **2020**, *21*, 376.
[19] Z. C. Xu, X. Y. Wang, H. Huang, *J. Appl. Polym. Sci.* **2020**, *137*, 48.
[20] Z. Z. Fang, N. Zheng, Q. Zhao, T. Xie, *ACS Appl. Mater. Interfaces* **2017**, *9*, 27.
[21] W. Z. Wang, W. Nie, D. H. Liu, H. B. Du, X. J. Zhou, L. Chen, H. S. Wang, X. M. Mo, L. Li, C. L. He, *Int. J. Nanomed.* **2018**, *13*, 7003.
[22] Y. F. Zhang, H. Z. Ying, K. R. Hart, Y. X. Wu, A. J. Hsu, A. M. Coppola, T. A. Kim, K. Yang, N. R. Sottos, S. R. White, J. J. Cheng, *Adv. Mater.* **2016**, *28*, 7646.
[23] L. H. Zhang, S. J. Rowan, *Macromolecules* **2017**, *50*, 5051.
[24] K. Ehrmann, S. Baudis, R. Liska, M. Fitzka, (Technische Universität Wien), *WO2022003204A1*, **2022**.
[25] H. Ying, Y. Zhang, J. Cheng, *Nat. Commun.* **2014**, *5*, 3218.
[26] S. Baudis, H. Bergmeister, K. Ehrmann, C. Grasl, R. Liska, B. Podesser, H. Schima, (Medizinische Universität Wien, Technische Universität Wien, Ludwig Boltzmann Gesellschaft- Österreichische Vereinigung zur Förderung der wissenschaftlichen Forschung), *WO2022162166A1*, **2022**.
[27] C. E. T. Stowell, X. Y. Li, M. H. Matsunaga, C. B. Cockreham, K. M. Kelly, J. Cheetham, E. Tzeng, Y. D. Wang, *J. Tissue Eng. Regener. Med.* **2020**, *14*, 1673.
[28] W. J. vanderGiessen, A. M. Lincoff, R. S. Schwartz, H. M. M. vanBeusekom, P. W. Serruys, D. R. Holmes, S. G. Ellis, E. J. Topol, *Circulation* **1996**, *94*, 1690.
[29] B. V. Udelsman, R. Khosravi, K. S. Miller, E. W. Dean, M. R. Bersi, K. Rocco, T. Yi, J. D. Humphrey, C. K. Breuer, *J. Biomech.* **2014**, *47*, 2070.
[30] C. L. Ives, J. L. Zamora, S. G. Eskin, D. G. Weilbaecher, Z. R. Gao, G. P. Noon, M. E. DeBakey, *Trans.- Am. Soc. Artif. Intern. Organs* **1984**, *30*, 587.
[31] R. Guidoin, M. Sigot, M. King, M. F. Sigotluizard, *Biomaterials* **1992**, *13*, 281.
[32] Z. Zhang, M. King, R. Guidoin, M. Therrien, C. Doillon, W. L. Diehljones, E. Huebner, *Biomaterials* **1994**, *15*, 1129.
[33] B. Huang, Y. Marois, R. Roy, M. Julien, R. Guidoin, *Biomaterials* **1992**, *13*, 209.
[34] Y. Marois, E. Paris, Z. Zhang, C. J. Doillon, M. W. King, R. G. Guidoin, *Biomaterials* **1996**, *17*, 1289.
[35] M. Ferraresso, S. Bertoli, P. Nobili, E. M. Bortolani, *J. Vasc. Access* **2013**, *14*, 252.
[36] M. Ferraresso, E. M. Bortolani, G. Amnon, *J. Vasc. Access* **2016**, *17*, 210.
[37] E. M. A. Christenson, J. M. Hiltner, *Corros. Eng., Sci. Technol.* **2007**, *42*, 312.
[38] V. S. Chernonosova, P. P. Laktionov, *Polymers* **2022**, *14*, 1698.
[39] G. Konig, T. N. McAllister, N. Dusserre, S. A. Garrido, C. Iyican, A. Marini, A. Fiorillo, H. Avila, W. Wystrychowski, K. Zagalski, M. Maruszewski, A. L. Jones, L. Cierpka, L. M. de la Fuente, N. L'Heureux, *Biomaterials* **2009**, *30*, 1542.

[40] N. L'Heureux, N. Dusserre, G. Konig, B. Victor, P. Keire, T. N. Wight, N. A. Chronos, A. E. Kyles, C. R. Gregory, G. Hoyt, R. C. Robbins, T. N. McAllister, *Nat. Med.* **2006**, *12*, 361.
[41] Y. Jeong, Y. Yao, E. K. F. Yim, *Biomater. Sci.* **2020**, *8*, 4383.
[42] A. Weekes, N. Bartnikowski, N. Pinto, J. Jenkins, C. Meinert, T. J. Klein, *Acta Biomater.* **2022**, *138*, 92.
[43] V. A. Kumar, L. P. Brewster, J. M. Caves, E. L. Chaikof, *Cardiovasc. Eng. Technol.* **2011**, *2*, 137.
[44] S. Roll, J. Muller-Nordhorn, T. Keil, H. Scholz, D. Eidt, W. Greiner, S. N. Willich, *BMC Surg.* **2008**, *8*, 22.
[45] N. L'Heureux, N. Dusserre, A. Marini, S. Garrido, L. de la Fuente, T. McAllister, *Nat. Clin. Pract. Cardiovasc. Med.* **2007**, *4*, 389.
[46] T. T. Lu, L. G. Yan, J. A. Madri, *Proc. Natl. Acad. Sci. USA* **1996**, *93*, 11808.
[47] P. J. Newman, D. K. Newman, *Arterioscler., Thromb., Vasc. Biol.* **2003**, *23*, 953.
[48] J. L. Snyder, E. McBeath, T. N. Thomas, Y. J. Chiu, R. L. Clark, K. Fujiwara, *Biol. Cell* **2017**, *109*, 312.
[49] V. B. Dugina, G. S. Shagieva, A. S. Shakhov, I. B. Alieva, *Int. J. Mol. Sci.* **2021**, *22*, 7836.
[50] D. Klein, *Stem Cells Int.* **2016**, *2016*, 1905846.
[51] W. D. Gu, X. C. Hong, C. Potter, A. J. Qu, Q. B. Xu, *Microcirculation* **2017**, *24*, 12324.
[52] N. F. Huang, S. Li, *Regen. Med.* **2008**, *3*, 877.
[53] K. Z. Tan, H. T. Zhu, J. F. Zhang, W. L. Ouyang, J. F. Tang, Y. M. Zhang, L. L. Qiu, X. Q. Liu, Z. P. Ding, X. M. Deng, *Stem Cells Int.* **2019**, *2019*, 8717694.
[54] K. Kawamoto, M. Konno, H. Nagano, S. Nishikawa, Y. Tomimaru, H. Akita, N. Hama, H. Wada, S. Kobayashi, H. Eguchi, M. Tanemura, T. Ito, Y. Doki, M. Mori, H. Ishii, *Dis. Markers* **2013**, *35*, 392578.
[55] T. Hollweck, M. Marschmann, I. Hartmann, B. Akra, B. Meiser, B. Reichart, M. Eblenkamp, E. Wintermantel, G. Eissner, *Biomed. Mater.* **2010**, *5*, 065004.
[56] M. Enayati, S. Puchhammer, J. Iturri, C. Grasl, C. Kaun, S. Baudis, I. Walter, H. Schima, R. Liska, J. Wojta, J. L. Toca-Herrera, B. K. Podesser, H. Bergmeister, *J. Mech. Behav. Biomed. Mater.* **2020**, *112*, 104077.
[57] K. R. Milner, A. J. Snyder, C. A. Siedlecki, *J. Biomed. Mater. Res., Part A* **2006**, *76a*, 561.
[58] L. S. Wan, Z. K. Xu, *J. Biomed. Mater. Res., Part A* **2009**, *89a*, 168.
[59] J. H. Lee, G. Khang, J. W. Lee, H. B. Lee, *J. Biomed. Mater. Res.* **1998**, *40*, 180.
[60] M. C. Belanger, Y. Marois, R. Roy, Y. Mehri, E. Wagner, Z. Zhang, M. W. King, M. J. Yang, C. Hahn, R. Guidoin, *Artif. Organs* **2000**, *24*, 879.
[61] J. Yi, M. C. Boyce, G. F. Lee, E. Balizer, *Polymer* **2006**, *47*, 319.
[62] H. Z. Ying, J. Yen, R. B. Wang, Y. Lai, J. L. A. Hsu, Y. H. Hu, J. J. Cheng, *Biomater. Sci.* **2017**, *5*, 2398.
[63] B. C. Yi, Y. B. Shen, H. Tang, X. L. Wang, B. Li, Y. Z. Zhang, *ACS Appl. Mater. Interfaces* **2019**, *11*, 6867.
[64] M. Eilenberg, M. Enayati, D. Ehebruster, C. Grasl, I. Walter, B. Messner, S. Baudis, P. Potzmann, C. Kaun, B. K. Podesser, J. Wojta, H. Bergmeister, *Eur. J. Vasc. Endovasc.* **2020**, *59*, 643.
[65] D. E. Heath, *Macromol. Chem. Phys.* **2017**, *218*, 8.
[66] L. Chang, M. T. Garcia-Barrio, Y. E. Chen, *Arterioscler., Thromb., Vasc. Biol.* **2020**, *40*, 1094.
[67] D. L. Brasaemle, *J. Lipid Res.* **2007**, *48*, 2547.
[68] E. J. Blanchettemackie, N. K. Dwyer, T. Barber, R. A. Coxey, T. Takeda, C. M. Rondinone, J. L. Theodorakis, A. S. Greenberg, C. Londos, *J. Lipid Res.* **1995**, *36*, 1211.
[69] L. Q. Zou, W. Y. Wang, S. X. Liu, X. J. Zhao, Y. Lyv, C. K. Du, X. Y. Su, B. Geng, G. H. Xu, *Biochim. Biophys. Acta, Mol. Basis Dis.* **2016**, *1862*, 182.
[70] L. Russo, C. N. Lumeng, *Immunology* **2018**, *155*, 407.
[71] H. Kane, L. Lynch, *Trends Immunol.* **2019**, *40*, 857.
[72] M. El Hafidi, M. Buelna-Chontal, F. Sanchez-Munoz, R. Carbo, *Int. J. Mol. Sci.* **2019**, *20*, 3657.
[73] Y. K. Lee, J. H. Sohn, J. S. Han, Y. J. Park, Y. G. Jeon, Y. Ji, K. T. Dalen, C. Sztalryd, A. R. Kimmel, J. B. Kim, *Diabetes* **2018**, *67*, 791.
[74] F. Zhang, M. W. King, *Adv. Healthcare Mater.* **2022**, *11*, 12.
[75] E. Arciniegas, L. M. Carrillo, J. B. De Sanctis, D. Candelle, *Cell Adhes. Migr.* **2008**, *2*, 17.
[76] B. Yang, W. Li, Q. C. Zheng, T. Qin, K. Wang, J. J. Li, B. Guo, Q. H. Yu, Y. Z. Wu, Y. Gao, X. Cheng, S. B. Hu, S. N. Kumar, S. G. Liu, Z. F. Song, *Biochem. Biophys. Res. Commun.* **2015**, *463*, 130.
[77] J. L. Johnson, A. Dwivedi, M. Somerville, S. J. George, A. C. Newby, *Arterioscler., Thromb., Vasc. Biol.* **2011**, *31*, E35.
[78] M. Steenport, K. M. F. Khan, B. H. Du, S. E. Barnhard, A. J. Dannenberg, D. J. Falcone, *J. Immunol.* **2009**, *183*, 8119.
[79] H. Bergmeister, C. Schreiber, C. Grasl, I. Walter, R. Plasenzotti, M. Stoiber, D. Bernhard, H. Schima, *Acta Biomater.* **2013**, *9*, 6032.
[80] S. Rohringer, K. H. Schneider, G. Eder, P. Hager, M. Enayati, B. Kapeller, H. Kiss, U. Windberger, B. K. Podesser, H. Bergmeister, *Mater. Today Bio* **2022**, *14*, 100262.
[81] M. Enayati, K. H. Schneider, C. Almeria, C. Grasl, C. Kaun, B. Messner, S. Rohringer, I. Walter, J. Wojta, L. Budinsky, B. H. Walpoth, H. Schima, G. Kager, S. Hallstrom, B. K. Podesser, H. Bergmeister, *Acta Biomater.* **2021**, *134*, 276.